

# REPORT DOCUMENTATION PAGE

Form Approved  
OMB No. 0704-0188

Public reporting burden for this collection of information is estimated to average 1 hour per response, including the time for reviewing instructions, searching existing data sources, gathering and maintaining the data needed, and completing and reviewing this collection of information. Send comments regarding this burden estimate or any other aspect of this collection of information, including suggestions for reducing this burden to Department of Defense, Washington Headquarters Services, Directorate for Information Operations and Reports (0704-0188), 1215 Jefferson Davis Highway, Suite 1204, Arlington, VA 22202-4302. Respondents should be aware that notwithstanding any other provision of law, no person shall be subject to any penalty for failing to comply with a collection of information if it does not display a currently valid OMB control number. **PLEASE DO NOT RETURN YOUR FORM TO THE ABOVE ADDRESS.**

1. REPORT DATE (DD-MM-YYYY)		2. REPORT TYPE Technical Paper		3. DATES COVERED (From - To)	
4. TITLE AND SUBTITLE				5a. CONTRACT NUMBER F64611-99-C-0018	
				5b. GRANT NUMBER	
				5c. PROGRAM ELEMENT NUMBER	
6. AUTHOR(S)				5d. PROJECT NUMBER 3005	
				5e. TASK NUMBER 0055	
				5f. WORK UNIT NUMBER	
7. PERFORMING ORGANIZATION NAME(S) AND ADDRESS(ES)  Busek				8. PERFORMING ORGANIZATION REPORT	
9. SPONSORING / MONITORING AGENCY NAME(S) AND ADDRESS(ES)  Air Force Research Laboratory (AFMC) AFRL/PRS 5 Pollux Drive Edwards AFB CA 93524-7048				10. SPONSOR/MONITOR'S ACRONYM(S)	
				11. SPONSOR/MONITOR'S NUMBER(S)	
12. DISTRIBUTION / AVAILABILITY STATEMENT  Approved for public release; distribution unlimited.					
13. SUPPLEMENTARY NOTES					
14. ABSTRACT  <div>20021202 092</div>					
15. SUBJECT TERMS					
16. SECURITY CLASSIFICATION OF:			17. LIMITATION OF ABSTRACT  A	18. NUMBER OF PAGES	19a. NAME OF RESPONSIBLE PERSON Leilani Richardson
a. REPORT Unclassified	b. ABSTRACT Unclassified	c. THIS PAGE Unclassified			19b. TELEPHONE NUMBER (include area code) (661) 275-5015

**Standard Form 298 (Rev. 8-98)**  
Prescribed by ANSI Std. Z39.18

1 item enclosed

3005005 J

MEMORANDUM FOR PRS (Contractor/In-House Publication)

FROM: PROI (STINFO)

12 October 2001

SUBJECT: Authorization for Release of Technical Information, Control Number: **AFRL-PR-ED-TP-2001-202**  
Peter S. Rostler (Busek), "A-I-D Time-Dependent Model of a Hall Thruster with Side Walls"

**International Electric Propulsion Conference**  
**Pasadena, CA (15 Oct 2001) – (Deadline: 15 Oct 01)**

**(Statement A)**

1. This request has been reviewed by the Foreign Disclosure Office for: a.) appropriateness of distribution statement, b.) military/national critical technology, c.) export controls or distribution restrictions, d.) appropriateness for release to a foreign nation, and e.) technical sensitivity and/or economic sensitivity.

Comments: \_\_\_\_\_  
\_\_\_\_\_  
\_\_\_\_\_

Signature \_\_\_\_\_ Date \_\_\_\_\_

2. This request has been reviewed by the Public Affairs Office for: a.) appropriateness for public release and/or b) possible higher headquarters review

Comments: \_\_\_\_\_  
\_\_\_\_\_  
\_\_\_\_\_

Signature \_\_\_\_\_ Date \_\_\_\_\_

3. This request has been reviewed by the STINFO for: a.) changes if approved as amended, b.) appropriateness of distribution statement, c.) military/national critical technology, d.) economic sensitivity, e.) parallel review completed if required, and f.) format and completion of meeting clearance form if required

Comments: \_\_\_\_\_  
\_\_\_\_\_  
\_\_\_\_\_

Signature \_\_\_\_\_ Date \_\_\_\_\_

4. This request has been reviewed by PRS for: a.) technical accuracy, b.) appropriateness for audience, c.) appropriateness of distribution statement, d.) technical sensitivity and economic sensitivity, e.) military/national critical technology, and f.) data rights and patentability

Comments: \_\_\_\_\_  
\_\_\_\_\_  
\_\_\_\_\_

APPROVED/APPROVED AS AMENDED/DISAPPROVED

\_\_\_\_\_  
PHILIP A. KESSEL Date  
Technical Advisor  
Space & Missile Propulsion Division

# A 1-D Time-Dependent Model of a Hall Thruster with Sides Walls

Peter S. Rostler  
Busek Co. Inc.  
11 Tech Circle  
Natick, MA 01760  
508-655-5565

IEPC-01-22

## Abstract

Previous one-dimensional Hall thruster models predict some observed features correctly, but do not adequately treat the losses of energy and ionization to the side walls of the channel. Because those losses have important effects on the discharge dynamics and the thruster's efficiency and lifetime, their omission severely limits the utility of a model. The model reported here is obtained from a two-dimensional description by solving analytically for the radial variations of densities and velocities and then averaging over the radial coordinate in a way that retains the effects of the side walls. Our model also includes ion pressure, second ionization, a varying electron temperature, a diverging channel and a non-radial  $B$  field. It calculates the ion flux into the walls as well as the incident ion angles and energies as functions of axial position to predict the profile of erosion of the walls by sputtering. The collision and ionization rates are all treated as functions of the electron temperature. The derivation of the equations is explained and typical results of numerical solutions are presented.

## 1.0 Introduction

Hall thrusters have been modeled numerically using 1-D fluid equations<sup>[1-6]</sup> and 2-D hybrid and particle descriptions.<sup>[7-14]</sup> To include enough particles for accurate predictions, the 2-D codes require long computations. The simpler 1-D models run faster and can therefore survey more cases, but the utility

of existing 1-D models is limited by their lack of an accurate treatment of the effects of the side walls of the channel, which are a sink for ionization and energy. Plasma recombines at the walls and the discharge electrons are cooled there by replacement of hot primaries with cold secondaries. These processes affect the discharge stability and the thruster efficiency.

To include side wall effects while retaining the simplicity of a 1-D computation, the model described here starts with a three-dimensional description and derives a 1-D approximation in a way that retains the side wall losses. The description is time-varying, includes a nonuniform electron temperature and second ionization, uses collision and ionization rates that depend upon  $T_e$  and allows the wall surface conductivity to limit the strength of the electric field. The model also includes ion pressure. The flow of plasma into the walls is driven by both the electron and ion pressures, so both are needed to calculate the wall recombination. Although one-dimensional, the model allows for a diverging channel and a  $B$  field that is not exactly radial. It calculates the ion flux into the walls as well as the incident ion angles and energies as a function of  $z$ , which can be used to predict the erosion of the walls by sputtering. This model assumes quasineutrality,  $n_e = n^+ + n^{++}$  or, including second ionization,

$$n_e = n^+ + 2 n^{++} \quad [1]$$

and it also assumes that the electron gyroradius is negligible compared to other distances in the problem. These two assumptions are checked during the computation.

Since the curvature in a thruster channel is small relative to its width, local Cartesian coordinates are used, as sketched below.

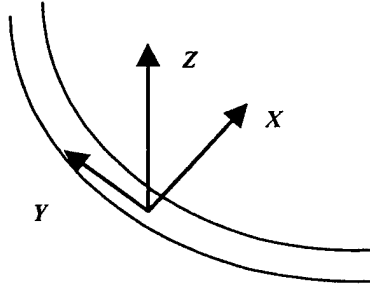


Figure 1 Coordinates

The axial (acceleration) direction is "z", the radial (across-channel) coordinate is "x" and the azimuth (with which nothing varies) is "y". The x-dependence is approximated analytically, leaving equations with two independent variables, z and t, that are solved numerically.

All 1-D and 2-D models assume azimuthal uniformity. In the early experiments on Hall thrusters, this was far from true. Probe measurements showed a rotating spike of density.<sup>[15]</sup> Later analysis concluded that to avoid or at least limit this instability one needs a negative axial gradient of (n/B).<sup>[16]</sup> Models like this one assume that this is done correctly. There may still be azimuthal waves and these can enhance the axial electron transport.<sup>[17,18]</sup> This increased conductivity is included in the model via the anomalous Hall parameter.

## 2.0 Ion and Neutral Dynamics

The ion dynamics are described by the Vlasov equations for singly and doubly charged xenon:

$$\frac{\partial f^+}{\partial t} + v_i \frac{\partial f^+}{\partial r_i} + \frac{e E_i}{M} \frac{\partial f^+}{\partial v_i} = \delta(v - v_0) n_0 \beta n_e - f^+ n_e \gamma \quad [2]$$

and

$$\frac{\partial f^{++}}{\partial t} + v_i \frac{\partial f^{++}}{\partial r_i} + \frac{2e E_i}{M} \frac{\partial f^{++}}{\partial v_i} = f^+ n_e \gamma \quad [3]$$

Here  $f=f(x, y, t)$  are the ion distributions; the subscript  $i=x, y$  and  $z$ ; a repeated index means a sum;  $n_e = n^+ + 2n^{++}$  is the electron density,  $n_0$  and  $v_0$  are the neutral density and velocity and  $e$  is the magnitude of the electronic charge\*. The right sides of the equations describe ion creation and loss by collisional ionization of neutral xenon and second ionization of xenon ions, with the temperature-dependent rates,  $\beta = \beta(T_e)$  and  $\gamma = \gamma(T_e)$ .

Making the usual definitions of density,  $n$ , velocity,  $u_i$ , pressure,  $P_{ij}$  and heat flux,  $Q_{ijk}$  in terms of velocity moments of the distribution function, one obtains fluid-type equations by taking moments of [2] and [3]. The only nonstandard elements are the source and sink terms.

Simple velocity integrals ("zeroth" moments) of [2] and [3] give continuity equations,

$$\frac{\partial n^+}{\partial t} + \frac{\partial}{\partial r_i} (n^+ u_i^+) = \beta n_0 n_e - \gamma n^+ n_e \quad [4]$$

$$\text{and} \quad \frac{\partial n^{++}}{\partial t} + \frac{\partial}{\partial r_i} (n^{++} u_i^{++}) = \gamma n^+ n_e \quad [5]$$

This is tensor notation, so a repeated index means a sum over three terms.

Taking the first moments, and using the continuity equations to simplify them gives momentum equations,

$$\begin{aligned} n^+ M \frac{\partial u_j^+}{\partial t} + n^+ M u_i^+ \frac{\partial u_j^+}{\partial r_i} \\ = e E_j n^+ - \frac{\partial P_{ij}^+}{\partial r_i} - \beta M n_e n_0 (u_j^+ - v_{0j}) \end{aligned} \quad [6]$$

and

\* This notation could be confusing. The subscript "i" doesn't mean "ion", it means x, y or z. Ion density, velocity, etc. are denoted by superscripts:  $n^+$ ,  $n^{++}$ ,  $u^+$ , etc. The ion velocity components  $u_i^+$  are functions of position, but the components of  $v_i$  in equations involving  $f$  are not — they are the other three coordinates of the six-dimensional phase space. Subscripts are used for electrons and neutrals:  $n_e$ ,  $n_0$ ,  $v_e$ ,  $v_0$ . Superscripts,  $n^-$ ,  $n^0$ , etc. would be more consistent with the ion terminology, but subscripts are more conventional.

$$n^{++}M \frac{\partial u_j^{++}}{\partial t} + n^{++}M u_i^{++} \frac{\partial u_j^{++}}{\partial r_i} \quad [7]$$

$$= 2eE_j n^{++} - \frac{\partial P_{ij}^{++}}{\partial r_i} - \gamma M n_e n^+ (u_j^{++} - u_j^+)$$

These each represent three equations,  $j = x, y$  and  $z$ .

Taking second moments of [2] and [3] and using [4]-[7] to simplify gives

$$\begin{aligned} \left( \frac{\partial}{\partial t} + u_i^+ \frac{\partial}{\partial r_i} + \gamma n_e \right) P_{jk}^+ + \frac{\partial Q_{jki}^+}{\partial r_i} + P_{jk}^+ \frac{\partial u_i^+}{\partial r_i} + P_{ki}^+ \frac{\partial u_j^+}{\partial r_i} + P_{ji}^+ \frac{\partial u_k^+}{\partial r_i} = \\ = n_0 n_e M \beta (u_j^+ - v_{0j})(u_k^+ - v_{0k}) \end{aligned} \quad [8]$$

and

$$\begin{aligned} \left( \frac{\partial}{\partial t} + u_i^{++} \frac{\partial}{\partial r_i} \right) P_{jk}^{++} + \frac{\partial Q_{jki}^{++}}{\partial r_i} + P_{jk}^{++} \frac{\partial u_i^{++}}{\partial r_i} + P_{ki}^{++} \frac{\partial u_j^{++}}{\partial r_i} + P_{ji}^{++} \frac{\partial u_k^{++}}{\partial r_i} = \\ = \gamma n_e P_{jk}^+ + n^+ n_e M \gamma (u_j^{++} - u_j^+)(u_k^{++} - u_k^+) \end{aligned} \quad [9]$$

These each represent nine equations.

This set has too many unknowns to solve. The usual simplification is to disregard the  $Q_{ijk}$ 's and replace the  $P_{ij}$ 's by scalar pressures:

$$P_{ij}^+ = \delta_{ij} p^+ \quad P_{ij}^{++} = \delta_{ij} p^{++} \quad [10]$$

Since collisions are insufficient to isotropize the pressures, this assumes that instabilities do so. That may not be true, but remember the objective, to include wall losses. The ion pressure comes from ions being made at different places and therefore falling through different voltage drops, creating a velocity spread — in the  $z$  direction. But the ion pressure that drives the flow into the walls is in the  $x$  direction. This pressure wouldn't even exist without collisions to isotropize the ions. So assuming a scalar pressure is the worst case, where the ions flow into the walls as fast as possible.

Assuming [10] and disregarding  $Q$  reduces all six off-diagonal ( $i \neq j$ ) equations [8] to

$$n_0 n_e M \beta (u_j^+ - v_{0j})(u_k^+ - v_{0k}) = 0$$

and all six off-diagonal equations [9] to

$$n^+ n_e M \gamma (u_j^{++} - u_j^+)(u_k^{++} - u_k^+) = 0$$

Since  $u_y^+ = v_{0y} = u_y^{++} = 0$ , these equations are trivially true for the four cases where either  $j$  or  $k$  is  $y$ , the azimuthal coordinate. The remaining two cases,  $j=x; k=z$  and  $j=z; k=x$  each give

$$n_0 n_e M \beta (u_x^+ - v_{0x})(u_z^+ - v_{0z}) = 0$$

for singly ionized and

$$n^+ n_e M \gamma (u_x^{++} - u_x^+)(u_z^{++} - u_z^+) = 0$$

for doubly ionized xenon. Since the  $z$  velocities are not zero, these equations are true only at the channel midplane, where the  $x$  velocities are zero. Everywhere else, the best one can say is that the  $x$  velocities are much smaller than the  $z$  velocities, and therefore are negligible.

The three remaining components of equation [8], namely  $i=j=x$  and  $i=j=y$  and  $i=j=z$ , are

$$\left(\frac{\partial}{\partial t} + u_i^+ \frac{\partial}{\partial r_i} + \gamma n_e\right) p^+ + p^+ \frac{\partial u_i^+}{\partial r_i} + 2p^+ \frac{\partial u_x^+}{\partial x} = n_0 n_e M \beta (u_x^+ - v_{0x})^2$$

$$\left(\frac{\partial}{\partial t} + u_i^+ \frac{\partial}{\partial r_i} + \gamma n_e\right) p^+ + p^+ \frac{\partial u_i^+}{\partial r_i} = 0$$

and

$$\left(\frac{\partial}{\partial t} + u_i^+ \frac{\partial}{\partial r_i} + \gamma n_e\right) p^+ + p^+ \frac{\partial u_i^+}{\partial r_i} + 2p^+ \frac{\partial u_z^+}{\partial z} = n_0 n_e M \beta (u_z^+ - v_{0z})^2$$

Adding these three equations gives

$$3 \left(\frac{\partial}{\partial t} + u_i^+ \frac{\partial}{\partial r_i} + \gamma n_e\right) p^+ + 5p^+ \frac{\partial u_i^+}{\partial r_i} = n_0 n_e M \beta [(u_x^+ - v_{0x})^2 + (u_z^+ - v_{0z})^2]$$

Using continuity [4] to eliminate the divergence of  $u^+$  gives

$$\begin{aligned} 3 \left(\frac{\partial}{\partial t} + u_i^+ \frac{\partial}{\partial r_i} + \gamma n_e\right) p^+ + \frac{5p^+}{n^+} (\beta n_0 n_e - \gamma n^+ n_e - u_i^+ \frac{\partial n^+}{\partial r_i} - \frac{\partial n^+}{\partial t}) = \\ = n_0 n_e M \beta [(u_x^+ - v_{0x})^2 + (u_z^+ - v_{0z})^2] \end{aligned}$$

which simplifies to

$$\begin{aligned} \left(\frac{\partial}{\partial t} + u_i^+ \frac{\partial}{\partial r_i}\right) \ln \left[ \frac{p^+}{(n^+)^{5/3}} \right] = \\ = \frac{n_0 n_e \beta}{3p^+ n^+} \left\{ M n^+ [(u_x^+ - v_{0x})^2 + (u_z^+ - v_{0z})^2] - 5p^+ \right\} - \gamma n_e \end{aligned} \quad [11]$$

The same calculations for equation [9] give, for the doubly-ionized xenon:

$$\begin{aligned} \left(\frac{\partial}{\partial t} + u_i^{++} \frac{\partial}{\partial r_i}\right) \ln \left[ \frac{p^{++}}{(n^{++})^{5/3}} \right] = \\ = \frac{n^+ n_e \gamma}{3p^{++} n^{++}} \left\{ M n^{++} [(u_x^{++} - u_x^+)^2 + (u_z^{++} - u_z^+)^2] - 5p^{++} + \frac{3p^+ n^{++}}{n^+} \right\} \end{aligned} \quad [12]$$

Equations [11] and [12] are only complicated because of the source terms. Assuming that  $\beta$  and  $\gamma$  are both zero collapses them to  $p/(n^{5/3}) = \text{constant}$ , the adiabatic equation of state.

Altogether, there are five equations for each species, a continuity equation [4] or [5] the three components of the momentum ( $F=Ma$ ) equation [6] or [7] and a pressure equation [11] or [12]. The latter required some approximations, but remember that the pressure is a small effect. Most 1-D models don't

even include ion pressure. It is included here because it affects the flow of plasma into the walls. However, because the ion pressure is a small effect, it doesn't have to be calculated as accurately as the other variables.

### 3.0 Quasi-One-D Trial Solution

To make a quasi-one-D approximation, we assume that nothing varies in the azimuthal ( $y$ ) direction and that the transverse ( $x$ ) expansion has the form,

$$u_x^+(x, z) = \tilde{u}_x^+(x) \cdot \tilde{u}_x^+(z) \quad [13]$$

and likewise for  $n^+$ ,  $u_x^{++}$ ,  $p^+$ , etc. To obtain a trial form for  $\tilde{u}_x^+(x)$  etc., we assume that the plasma expands uniformly and impinges on the wall at the plasma sound speed,  $v_s$ . This is consistent with the Bohm sheath criterion that plasma enters sheaths at  $v_s$  or faster. Otherwise, a precursor sheath — a rarefaction fan — forms to accelerate plasma into the sheath.

The problem is complicated by the two ion species. The usual sound speed is  $v_s \equiv \sqrt{k(T_e + T_i)/M}$ . A generalization is

$$\begin{aligned} v_s^+ &\equiv \sqrt{\frac{n^+ k T_e + p^+}{n^+ M}} \\ v_s^{++} &\equiv \sqrt{\frac{2n^{++} k T_e + p^{++}}{n^{++} M}} \end{aligned} \quad [14]$$

The singly-charged xenon ions reach the wall at  $v_s^+$  while the doubly-charged ions reach the wall at  $v_s^{++}$ . This is an approximation. In a plasma with several species of ion, there are several sound speeds, but each species's speed involves the other species. However, these forms provide an overall pressure balance:

$$n^+ M (v_s^+)^2 + n^{++} M (v_s^{++})^2 = n_e k T_e + p^+ + p^{++}$$

and, in the limit of negligible ion pressures, they approach  $v_s^{++} = \sqrt{2} v_s^+$  as they should, since then the ions are all accelerated through the same  $E$  field.

Now assume that both species expand uniformly in the transverse direction:

$$\tilde{u}_x^+ = \frac{2v_s^+}{W} \cdot x \quad \tilde{u}_x^{++} = \frac{2v_s^{++}}{W} \cdot x \quad [15]$$

where  $W$  is the channel width. In these coordinates, the origin is at the center of the channel and the walls are at  $x = \pm W/2$ . In general,  $W$  will be an increasing function of  $z$  because the channel diverges.

Simplified versions of the force equations, [6] and [7] are

$$M \tilde{n}^+ \tilde{u}_x^+ \frac{\partial \tilde{u}_x^+}{\partial x} = -k(T_e + T^+) \frac{\partial \tilde{n}^+}{\partial x} \quad [16]$$

and

$$M \tilde{n}^{++} \tilde{u}_x^{++} \frac{\partial \tilde{u}_x^{++}}{\partial x} = -k(2T_e + T^{++}) \frac{\partial \tilde{n}^{++}}{\partial x} \quad [17]$$

Here  $\tilde{n}$  and  $\tilde{u}_x$  are functions of  $x$  and the  $T$ 's are constants. Substituting [13]--[15] into [16] and [17] gives,

$$\tilde{n}^+ = n_0^+ e^{-\frac{2x^2}{W^2}} \quad [18]$$

and

$$\tilde{n}^{++} = n_0^{++} e^{-\frac{2x^2}{W^2}}$$

So in the  $x$ -momentum equation, a linear acceleration implies a Gaussian density profile. Since the walls are at  $x = \pm W/2$ , the density at the walls is  $e^{-0.5} \approx 0.6$  times that in the center of the channel. Incorporating the  $n_0$ 's into the  $z$ -dependent parts, [18] gives the trial forms,

$$n^+(x, z, t) = \tilde{n}^+(z, t) e^{-\frac{2x^2}{W^2}} \quad [19]$$

$$n^{++}(x, z, t) = \tilde{n}^{++}(z, t) e^{-\frac{2x^2}{W^2}} \quad [20]$$

So  $\tilde{n}(z)$  is the density at  $x = 0$ , at the midplane. Quasineutrality gives the electron density:

$$n_e(x, z, t) = [\tilde{n}^+(z, t) + 2\tilde{n}^{++}(z, t)] e^{-\frac{2x^2}{W^2}} \quad [21]$$

Assuming that the  $x$ -components of velocity depend only upon  $x$ , and the  $z$ -components depend only upon  $z$ , gives,

$$u_x^+(x, z, t) = \tilde{u}_x^+(x, t) = \frac{2v_s^+}{W} \cdot x \quad [22]$$

$$u_z^+(x, z, t) = \tilde{u}_z^+(z, t)$$

$$u_x^{++}(x, z, t) = \tilde{u}_x^{++}(x, t) = \frac{2v_s^{++}}{W} \cdot x \quad [23]$$

$$u_z^{++}(x, z, t) = \tilde{u}_z^{++}(z, t)$$

$$\begin{aligned} p^+(x, z, t) &= n^+(x, z, t) k T^+(z, t) \\ p^{++}(x, z, t) &= n^{++}(x, z, t) k T^{++}(z, t) \end{aligned} \quad [24]$$

So the pressure is obtained from density and temperature (i.e. [24] defines the ion temperatures). The density is described by [19] or [20] and the ion temperature is assumed to vary only with  $z$ , not  $x$ .

Finally, for the pressures, the simplest assumption is

#### 4.0 Quasi-One-D Derivation

The goal now is to substitute these forms into the 3-D equations to get a one-D description. Logically, Eqs. [19]—[24] are guesses. If they didn't lead to approximately one-D equations, one would have to try different forms. But as will be seen, very little further approximation is necessary.

Using [19] and [22] in the continuity equation [4] gives

$$\frac{\partial \tilde{n}^+}{\partial t} + \frac{\partial}{\partial z} \left( \tilde{n}^+ \tilde{u}_z^+ \right) = \left( \beta n_0 - \gamma \tilde{n}^+ e^{-\frac{2x^2}{W^2}} \right) \left( \tilde{n}^+ + 2\tilde{n}^{++} \right) - \tilde{n}^+ \frac{2v_s^+}{W} \left( 1 - \frac{4x^2}{W^2} \right) \quad [25]$$

which is almost  $x$ -independent. Only the last two terms still vary with  $x$ , and that variation can be eliminated by averaging over the channel or, even simpler, by considering only the midplane,  $x=0$ . Notice that if one just wrote down one-D equations, one would assume a continuity equation similar to this -- except for the last term, which is new. This negative term is an additional loss. It accounts for the loss of plasma to the side walls of the channel.

Inserting the assumed forms into equation [5], the continuity equation for the doubly-ionized species gives a similar result,

$$\frac{\partial \tilde{n}^{++}}{\partial t} + \frac{\partial}{\partial z} \left( \tilde{n}^{++} \tilde{u}_z^{++} \right) = \gamma \tilde{n}^+ \left( \tilde{n}^+ + 2\tilde{n}^{++} \right) e^{-\frac{2x^2}{W^2}} - \tilde{n}^{++} \frac{2v_s^{++}}{W} \left( 1 - \frac{4x^2}{W^2} \right) \quad [26]$$

The momentum equations, [6] and [7] have three components, but the  $y$  components are trivial. Assuming that nothing varies with  $y$ , these just give  $\theta=0$ . The  $x$  component of Eq. [6] gives

$$\frac{2xM}{W} \frac{\partial v_s^+}{\partial t} + \frac{4kT_e x}{W^2} = eE_x - \frac{\beta M \left( \tilde{n}^+ + 2\tilde{n}^{++} \right) n_0}{\tilde{n}^+} \left( \frac{2v_s^+}{W} x - v_{0x} \right)$$

Neglecting the first term, which depends on the time variation of the temperature, one can regard the rest as specifying the ambipolar E-field:

$$\frac{eE_x}{M} = \frac{4x}{W^2} \frac{kT_e}{M} + \frac{\beta \left( \tilde{n}^+ + 2\tilde{n}^{++} \right) n_0}{\tilde{n}^+} \left( \frac{2v_s^+}{W} x - v_{0x} \right) \quad [27]$$



Since we are only interested in the  $z$ -dependence, we don't really need this equation, except to check for accuracy of the model. (If  $E_x > E_z$ , then the problem really isn't quasi-one-dimensional.) This is fortunate, because the  $x$ -component of [7], the momentum equation for the doubly-ionized species, gives a slightly different equation for the ambipolar  $E$  field:

$$\frac{eE_x}{M} = \frac{4x}{W^2} \frac{kT_e}{M} + \frac{\gamma(\tilde{n}^+ + 2\tilde{n}^{++})}{2\tilde{n}^{++}} \tilde{n}^+ \left( \frac{2x}{W} \right) (v_s^{++} - v_s^+) e^{-\frac{2x^2}{W^2}} \quad [28]$$

Making the quasi-one-D assumptions in the  $z$ -component of [6] gives,

$$\frac{\partial \tilde{u}_z^+}{\partial t} + \tilde{u}_z^+ \frac{\partial \tilde{u}_z^+}{\partial z} = \frac{eE_z}{M} - \frac{k}{M} \frac{\partial T^+}{\partial z} - \frac{kT^+}{M\tilde{n}^+} \frac{\partial \tilde{n}^+}{\partial z} - \frac{\beta(\tilde{n}^+ + 2\tilde{n}^{++})}{\tilde{n}^+} n_0 (\tilde{u}_z^+ - v_{0z}) \quad [29]$$

Except for a possible effect of  $n_0$ , this has no  $x$ -variation at all.

The  $z$ -component of [7] the momentum equation for the doubly-ionized species is,

$$\begin{aligned} \frac{\partial \tilde{u}_z^{++}}{\partial t} + \tilde{u}_z^{++} \frac{\partial \tilde{u}_z^{++}}{\partial z} = & \frac{2eE_z}{M} - \frac{k}{M} \frac{\partial T^{++}}{\partial z} - \frac{kT^{++}}{M\tilde{n}^{++}} \frac{\partial \tilde{n}^{++}}{\partial z} \\ & - \frac{\gamma(\tilde{n}^+ + 2\tilde{n}^{++})}{\tilde{n}^{++}} \tilde{n}^+ (\tilde{u}_z^{++} - \tilde{u}_z^+) e^{-\frac{2x^2}{W^2}} \end{aligned} \quad [30]$$

This too is almost completely independent of  $x$ . The only remaining  $x$  variation is in the last term (the momentum change due to production of  $\text{Xe}^{++}$  by second ionization of  $\text{Xe}^+$ ), and this  $x$ -dependence is easily eliminated by looking at the center of the channel. Again, the result is not very different from what one would get by merely writing down a one-D description, except that it now includes a drag due to ion creation.

So far, the quasi-static approximation has been surprisingly successful. The assumption of a uniform expansion in  $x$ , plus the Gaussian density profiles that match such an expansion has essentially eliminated the  $x$ -dependence, leaving equations that depend only on  $z$  and  $t$ . All that remains is to approximate the pressure equations.

Eq. [11], the pressure equation for the singly-ionized xenon gives,

$$\begin{aligned} \left[ \frac{\partial}{\partial t} + \tilde{u}_z^+ \frac{\partial}{\partial z} \right] \ln \left( \frac{kT^+}{(\tilde{n}^+)^{2/3}} \right) = & -\frac{16v_s^+ x^2}{3W^2} - \gamma(\tilde{n}^+ + 2\tilde{n}^{++}) e^{-\frac{2x^2}{W^2}} \\ & + \frac{Mn_0\beta}{3kT^+} \left( 1 + \frac{2\tilde{n}^{++}}{\tilde{n}^+} \right) \left[ \left( \frac{2v_s^+ x}{W} - v_{0x} \right)^2 + (u_z^+ - v_{0z})^2 - \frac{5kT^+}{M} \right] \end{aligned} \quad [31]$$

the  $x$ -dependence has certainly not disappeared here, but there is no reason why it should. The assumed  $x$ -variations of velocity and density were chosen to simplify the continuity and momentum equations, not this equation. But notice that the left hand side is independent of  $x$  and the right side can be greatly simplified by looking only at  $x=0$ .

Inserting the quasi-one-dimensional forms into [12], the pressure equation for doubly-ionized xenon gives,

$$\left[ \frac{\partial}{\partial t} + \tilde{u}_z^{++} \frac{\partial}{\partial z} \right] \ln \left( \frac{kT^{++}}{(\tilde{n}^{++})^{2/3}} \right) = - \frac{16v_s^{++} x^2}{3W^3} \quad [32]$$

$$+ \frac{M(\tilde{n}^+ + 2\tilde{n}^{++})\tilde{n}^+ \gamma}{3kT^{++}\tilde{n}^{++}} e^{\frac{2x^2}{W^2}} \left[ \frac{4x^2}{W^2} (v_s^{++} - v_s^+)^2 + (u_z^{++} - u_z^+)^2 - \frac{5kT^{++}}{M} + \frac{3kT^+}{M} \right]$$

This equation is similar to [31] but simpler, because there is no collisional loss of these ions. It also simplifies at  $x=0$ . This completes the model of the ion dynamics.

Restating the whole set of ion equations for flow along the midplane of the channel,  $x=0$  gives equations that depend only on  $z$  and  $t$ , as intended. From [25], the continuity equation for  $\text{Xe}^+$ , we have

$$\frac{\partial \tilde{n}^+}{\partial t} + \frac{\partial}{\partial z} (\tilde{n}^+ \tilde{u}_z^+) = (\beta n_0 - \gamma \tilde{n}^+) (\tilde{n}^+ + 2\tilde{n}^{++}) - \frac{2v_s^+ \tilde{n}^+}{W} \quad [33]$$

And [26] at  $x=0$  gives the continuity equation for  $\text{Xe}^{++}$ ,

$$\frac{\partial \tilde{n}^{++}}{\partial t} + \frac{\partial}{\partial z} (\tilde{n}^{++} \tilde{u}_z^{++}) = \gamma \tilde{n}^+ (\tilde{n}^+ + 2\tilde{n}^{++}) - \frac{2v_s^{++} \tilde{n}^{++}}{W} \quad [34]$$

The momentum equations were essentially independent of  $x$  as obtained already. From [29] we have, for the singly-ionized xenon,

$$\frac{\partial \tilde{u}_z^+}{\partial t} + \tilde{u}_z^+ \frac{\partial \tilde{u}_z^+}{\partial z} = \frac{eE_z}{M} - \frac{k}{M} \frac{\partial T^+}{\partial z} - \frac{kT^+}{M \tilde{n}^+} \frac{\partial \tilde{n}^+}{\partial z} - \frac{\beta (\tilde{n}^+ + 2\tilde{n}^{++}) \tilde{n}_0}{\tilde{n}^+} (\tilde{u}_z^+ - \tilde{v}_{0z}) \quad [35]$$

The only change from [29] is that the neutral density and velocity have been decorated with double tildes to signify that any  $x$ -variation in them has been eliminated by taking the values at the midplane of the channel.

Equation [30] taken at  $x=0$  gives the one-D momentum equation for the doubly-ionized xenon,

$$\frac{\partial \tilde{u}_z^{++}}{\partial t} + \tilde{u}_z^{++} \frac{\partial \tilde{u}_z^{++}}{\partial z} = \frac{2eE_z}{M} - \frac{k}{M} \frac{\partial T^{++}}{\partial z} - \frac{kT^{++}}{M \tilde{n}^{++}} \frac{\partial \tilde{n}^{++}}{\partial z} - \frac{\gamma (\tilde{n}^+ + 2\tilde{n}^{++}) \tilde{n}^+}{\tilde{n}^{++}} (\tilde{u}_z^{++} - \tilde{u}_z^+) \quad [36]$$

From [31] we have the equation for the pressure --- i.e. for the temperature --- of the singly-ionized xenon at the midplane,

$$\left[ \frac{\partial}{\partial t} + \tilde{u}_z^+ \frac{\partial}{\partial z} \right] \ln \left( \frac{kT^+}{(\tilde{n}^+)^{2/3}} \right) =$$

$$= \frac{M \tilde{n}_0 \beta}{3kT^+} \left( 1 + \frac{2\tilde{n}^{++}}{\tilde{n}^+} \right) \left[ (\tilde{u}_z^+ - \tilde{v}_{0z})^2 - \frac{5kT^+}{M} \right] - \gamma (\tilde{n}^+ + 2\tilde{n}^{++}) \quad [37]$$

Finally, [32] at  $x=0$  gives a similar equation for the temperature of the  $\text{Xe}^{++}$ ,

$$\left[ \frac{\partial}{\partial t} + \tilde{u}_z^{++} \frac{\partial}{\partial z} \right] \ln \left( \frac{kT^{++}}{(\tilde{n}^{++})^{2/3}} \right) =$$

$$= \frac{M(\tilde{n}^+ + 2\tilde{n}^{++})\tilde{n}^+\gamma}{3kT^{++}\tilde{n}^{++}} \left[ (\tilde{u}_z^{++} - \tilde{u}_z^+)^2 - \frac{5kT^{++}}{M} + \frac{3kT^+}{M} \right] \quad [38]$$

These six equations give the ion dynamics. Since there are six variables, namely the densities,  $z$ -velocities and temperatures of the two species, six equations are enough. These equations do not explicitly include energy equations for the ions, but these are implied and can be derived from the foregoing results. But because the energy equations are more complicated, it makes sense to use the above forms.

Remember that these final results are all at the midplane of the channel, in the quasi-one-dimensional approximation, [19] — [24]. So the total flux per unit circumference is not  $nu_z W$ , but

$$\text{Flux} = \int_{-W/2}^{W/2} \tilde{n} e^{-\frac{2x^2}{W^2}} \tilde{u}_z dx = \sqrt{2} W \tilde{n} \tilde{u}_z \int_0^{\frac{1}{\sqrt{2}}} e^{-\xi^2} d\xi =$$

$$= W \tilde{n} \tilde{u}_z \sqrt{\frac{\pi}{2}} \text{erf}\left(\frac{1}{\sqrt{2}}\right) = 0.86 W \tilde{n} \tilde{u}_z \quad [39]$$

The density at the midplane is  $\tilde{n}$ , the density at the walls was shown by Eq. [18] to be  $0.6\tilde{n}$  and Eq. [39] shows that the mean density averaged across the channel is  $0.86\tilde{n}$ .

This completes the model of the ion dynamics. The equations that describe the other species in the plasma, the electrons and the neutrals will be considered only in their one-dimensional forms along the midplane. Since all the quantities in the following equations refer to the midplane, the double tildes will be omitted from here on.

## 5.0 Neutrals

The equation of continuity for the neutral gas is

$$\frac{\partial n_0}{\partial t} + \frac{\partial}{\partial z}(n_0 v_{0z})$$

$$= -\beta n_0 (n^+ + 2n^{++}) + \frac{2(v_s^+ n^+ + v_s^{++} n^{++})}{W} \quad [40]$$

The last term describes neutrals coming off the wall where plasma has recombined. For consistency, the neutral density distribution in  $x$  is assumed to be Gaussian too. This conserves particles both along the centerline and across the channel. But it is an approximation. Because neutrals are coming off the walls, and because the rate of loss by ionization is greatest in the center where the plasma density is

highest, the neutral density really peaks at the edges of the channel, but modeling that correctly would require a full two-D analysis. Putting too many neutrals in the center, which this does, makes the ionization rate too high. To compensate for this, the ionization cross section could be reduced.

Since neutral-ion collisions are rare, the neutrals diffuse along the channel, colliding only with the walls. For a small density gradient,  $\frac{1}{n_0} \frac{\partial n_0}{\partial z} \leq \frac{1}{W}$ ,

the neutral velocity is

$$v_{0D} = -\frac{W}{3n_0} \frac{\partial n_0}{\partial z} v_{0S} \quad [41]$$

where

$$v_{0S} = \sqrt{\frac{kT_0}{M}} \quad [42]$$

and the neutral gas temperature  $T_0$  is constant.

For sharp density gradients, the velocity defined by [41] becomes much greater than the thermal velocity, which is unrealistic. To avoid this, the neutral velocity will be estimated as

$$v_{0z} = \left[ v_{0D}^{-1} + \left( \frac{-\frac{\partial n_0}{\partial z}}{\left| \frac{\partial n_0}{\partial z} \right|} v_{0S} \right)^{-1} \right]^{-1} \quad [43]$$

$$= v_{0S} \frac{-\frac{\partial n_0}{\partial z}}{\frac{3n_0}{W} + \left| \frac{\partial n_0}{\partial z} \right|}$$

which approaches  $v_{0D}$  for weak gradients and approaches  $v_{0S}$  for strong gradients.

## 6.0 Electron Dynamics

The electron density is determined by quasineutrality, Eq. [1]. The electron axial velocity is the collisional drift across the B-field due to the electric field and the pressure gradient:

$$v_{ez}^{(classical)} = -\frac{1}{B} \left[ E + \frac{1}{en_e} \frac{\partial(n_e k T_e)}{\partial z} \right] \frac{\nu_1 + \nu_2}{\Omega_e}$$

where  $\nu_1$  and  $\nu_2$  are elastic and inelastic collision frequencies and  $\Omega_e = \frac{eB}{m_e}$  is the electron

gyrofrequency. The ratio  $(\nu_1 + \nu_2)/\Omega_e$  is the reciprocal of the Hall parameter. This is the same equation used in other models,<sup>[2]</sup> except that here it is in SI units.

The Hall parameter may be either classical or anomalous. Considering  $\nu_1$  and  $\nu_2$  to be the classical collision frequencies, one knows that Hall thrusters can operate in regimes where this would give an unrealistically high Hall parameter. In that case, plasma fluctuations (e.g. azimuthal waves) that scatter electrons across the magnetic field will be the primary cause of electron current. This can be included in the theory by assuming an anomalous

Hall parameter,  $H_P$ , and writing the electron velocity as

$$v_{ez} = -\frac{1}{B} \left[ E + \frac{1}{en_e} \frac{\partial(n_e k T_e)}{\partial z} \right] \left[ \left( \frac{\nu_1 + \nu_2}{\Omega_e} \right)^2 + \frac{1}{(H_P)^2} \right]^{-\frac{1}{2}} \quad [44]$$

The electrons also satisfy a continuity equation,

$$\frac{\partial n_e}{\partial t} + \frac{\partial}{\partial z} (n_e v_{ez}) = (\beta n_0 + \gamma n^+) n_e - \frac{2}{W} (v_s^+ n^+ + 2 v_s^{++} n^{++}) \quad [45]$$

Since the electron density is determined by quasineutrality, this is a constraint on the electron velocity, and therefore, through Eq. [44], on the electric field.

## 7.0 Collisions

The ionization rate  $\beta$ , the second ionization rate  $\gamma$  and the electron elastic ( $\nu_1$ ) and inelastic ( $\nu_2$ ) collision frequencies are all functions of the electron temperature  $T_e$ . Fortunately, some data are available for the energy range of interest.<sup>[19]</sup> The simplest procedure is to approximate these data with empirical formulas.

The elastic collision frequency,  $\nu_1$ , is the sum of the frequency of collisions with neutral atoms, singly-charged ions, and with doubly-charged ions,

$$\nu_1 = R_{10} n_0 + R_1^+ n^+ + R_1^{++} n^{++} \quad [46]$$

$R_{10}$  is the rate for electron collisions with neutrals and  $R_1^+$  and  $R_1^{++}$  are the Coulomb collision rates.

The electron inelastic collision frequency also includes collisions with neutrals and with singly and doubly charged ions:

$$\nu_2 = \frac{R_{20} n_0 + R_2^+ n^+ + R_2^{++} n^{++}}{k T_e} \quad [47]$$

So one needs either tables or formulas for eight functions, namely the two ionization rates,  $\beta(T_e)$  and  $\gamma(T_e)$  (in  $m^3/s$ ), the three elastic collision rates,  $R_{10}(T_e)$ ,  $R_1^+(T_e)$  and  $R_1^{++}(T_e)$  (also in  $m^3/s$ ), and the

three inelastic rates,  $R_{20}(T_e)$ ,  $R_2^+(T_e)$  and  $R_2^{++}(T_e)$  (in  $W\text{-}m^3$ ).

## 8.0 Side Wall Boundary Conditions

If the walls are not conductive, the net current into the walls must vanish, so the electron and ion wall fluxes,  $\Gamma_e$ ,  $\Gamma^+$  and  $\Gamma^{++}$  have to balance:

$$\Gamma_e = \Gamma^+ + 2\Gamma^{++} + \delta\Gamma_e$$

where  $\delta = \delta(T_e)$  is the wall's electron secondary emission coefficient. Since the electron thermal velocity is higher than that of the ions, the electron flux would be greater, unless balanced by secondary emission or reduced by a sheath voltage barrier. The ion fluxes are

$$\Gamma^+ = 0.6n^+v_s^+ \quad \Gamma^{++} = 0.6n^{++}v_s^{++}$$

The factors of 0.6 enter because the densities at the channel edge are only 0.6 times those in the center where  $n^+$  and  $n^{++}$  are defined. According to the analysis of the MIT group<sup>[6]</sup> the primary electron flux into the wall is

$$\Gamma_e = 0.6(n^+ + 2n^{++}) \frac{c_e}{4} e^{\frac{e\Phi_w}{kT_e}} \quad [48]$$

where  $\Phi_w$  is the sheath voltage (negative because the electric field points toward the wall),  $c_e$  is the mean electron thermal speed<sup>[20]</sup>:

$$c_e = \sqrt{\frac{8kT_e}{\pi m_e}} \quad [49]$$

and  $m_e$  is the electron mass.

The effective secondary emission coefficient,  $\delta_{eff}$  is derived in Ref. 6 to be

$$\delta = \Gamma(2+B)A_0 \left( \frac{T_e}{11,600} \right)^{B_0} = 0.198 \left( \frac{T_e}{11,600} \right)^{0.576} \quad [50]$$

where  $A_0=0.141$  and  $B_0=0.576$  for boron nitride and  $\Gamma(x)$  is the Gamma function.

Solving these equations gives the sheath voltage:

$$\Phi_w = \frac{kT_e}{e} \ln \left( \frac{4n^+v_s^+ + 8n^{++}v_s^{++}}{c_e(1-\delta)(n^+ + 2n^{++})} \right) \quad [51]$$

If the ion temperatures are negligible,  $v_s^+ = v_s^{++}$  and Eq. [61] reduces to

$$\Phi_w = \frac{kT_e}{e} \ln \left( \frac{4v_s^+}{c_e(1-\delta)} \right) \quad [52]$$

Given the two densities and the three temperatures, Eq. [51] predicts the sheath voltage. Because  $c_e \gg v_s^+, v_s^{++}$ , the argument of the logarithm is much less than one and the sheath voltage is negative — unless the secondary coefficient  $\delta$  is nearly one. A negative voltage means the  $E$  field points toward the wall.

Eq. [50] says that  $\delta$  goes to one as the temperature approaches  $1.93 \times 10^5$  °K, which is 16.64 eV. At a slightly lower temperature the argument of the logarithm in Eq. [51] becomes one, driving the sheath voltage,  $\Phi_w$  to zero. One does not expect  $T_e$  to get this high because secondary emission cools the electrons by replacing hot primaries with cold secondaries. Indeed, this entire description is valid only if the sheath voltage  $\Phi_w$  is negative.

Ions strike the wall with the kinetic energy they had upon reaching the sheath, plus the energy gained by falling through the sheath. For singly-ionized xenon, this energy is,

$$V_w^+ = \frac{1}{2}M(v_s^+)^2 + e\Phi_w + \frac{1}{2}M(u_z^+)^2 \quad [53]$$

and doubly-ionized xenons strike the wall with energy,

$$V_w^{++} = \frac{1}{2}M(v_s^{++})^2 + 2e\Phi_w + \frac{1}{2}M(u_z^{++})^2 \quad [54]$$

These energies and the fluxes  $\Gamma^+$  and  $\Gamma^{++}$  can be used to estimate the erosion of the wall by sputtering. But this picture assumes that the acceleration of ions by the discharge voltage is precisely tangential to the wall, which is true only if

the  $B$  field is exactly radial. In reality, the  $B$ -field lines are curved, so even if the discharge  $E$  is normal to  $B$ , it can drive ions toward or away from the walls. But as discussed below, the model can be corrected for this effect.

## 9.0 Electron Temperature

The only piece still missing is the calculation of  $T_e$ . This must be obtained from the electron energy balance, the requirement that the change in the electron heat content equals the heating minus the cooling. In fact, the heat content is negligible, so the electron temperature must be whatever makes the heating and cooling almost equal, but for computation, it is simpler to use the energy equation. The heating equals the electric field times the electron current. Cooling is by inelastic collisions and by heat loss to the walls, where hot primaries are replaced by cold secondaries.

For wall cooling to affect  $T_e$  near channel center, the heat must conduct through the plasma. For thruster conditions, Spitzer's result<sup>[21]</sup> for the thermal conductivity of the plasma gives

The collisional power loss is quadratic in the density:

$$\begin{aligned} q_{coll} &= \nu_2 k T_e (n^+ + 2n^{++}) \int_{-W/2}^{W/2} \left( e^{-\frac{2x^2}{W^2}} \right)^2 dx = \\ &= \nu_2 k T_e (n^+ + 2n^{++}) W \int_0^1 e^{-\xi^2} d\xi = 0.75 \nu_2 k T_e (n^+ + 2n^{++}) W \end{aligned} \quad [57]$$

where  $\nu_2$  is the inelastic collision rate.

The electron energy loss to the walls is shown in Ref. 6 to be

$$q_{wall} = 2\Gamma_e [2k(T_e - \delta T_{sec}) - (1 - \delta)e\Phi_W] \quad [58]$$

where  $T_{sec}$  is the temperature of the emitted secondary electrons (approximately 1 eV) and a factor of two has been added to the result in Ref. 6 to account for the loss to both the inner and outer walls. Note that  $q_{in}$ ,  $q_{coll}$ , and  $q_{wall}$  are all in W/m<sup>2</sup>.

Using these in Eq. [55] gives an equation for electron temperature:

$K = 1.7 \cdot 10^{-13} T_e^{5/2}$  W/cm-deg. For the conditions in a Hall thruster, this keeps  $T_e$  quite uniform across the channel. The electron temperature is therefore determined by the energy balance, integrated across the channel

$$0.86 W \left( \frac{\partial}{\partial t} + v_e \frac{\partial}{\partial z} \right) \left( \frac{3}{2} n_e k T_e \right) = q_{in} - q_{coll} - q_{wall} \quad [55]$$

where  $q_{in}$  is the electrical power input to the electrons,  $q_{coll}$  is the power lost by inelastic collisions with atoms and ions, both integrated across the channel, and  $q_{wall}$  is the power lost to the walls. All three of these  $q$ 's vary with the electron temperature.

Integrating across the channel, as in Eq. [39] gives the power input:

$$q_{in} = -0.86 W (n^+ + 2n^{++}) e v_{ez} E \quad [56]$$

Here  $v_{ez}$  is the electron cross-field drift velocity given by Eq. [44] which does depend on  $T_e$ .

$$\frac{1}{n_e} \left( \frac{\partial}{\partial t} + v_e \frac{\partial}{\partial z} \right) \left( \frac{3}{2} n_e k T_e \right) = -e v_{ez} E - 0.87 v_2 k T_e \quad [59]$$

$$- 0.35 \frac{c_e}{W} e^{\frac{e\Phi_w}{kT_e}} [2k(T_e - \delta T_{sec}) - (1 - \delta) e\Phi_w]$$

Besides the explicit  $T_e$  dependence here, the drift velocity,  $v_{ez}$  (Eq. [44]), the thermal velocity  $c_e$  (Eq. [50]) the wall sheath potential,  $\Phi_w$  (Eq. [52]) and the secondary emission coefficient,  $\delta$  (Eq. [50]) are all functions of  $T_e$ .

For a numerical solution, this can be simplified, because the electron heat capacity is small compared to the heating and cooling rates. Physically,  $T_e$  assumes the value that makes the net heating (the rhs of this equation) vanish. Eq. [59] is simply a way to find that temperature. To avoid introducing shorter times and higher velocities into the calculation, the heat convection was omitted and the heat capacity artificially increased in the computations.

### 10.0 Non-Axial Flow, Non-Constant Width

With the foregoing equation for electron temperature, the model is complete. However, as now formulated it contains an inaccuracy that would limit its utility, namely the assumption that the walls are straight and  $B$  is normal to the walls. Where  $B$ -field lines bow outward, an  $E$ -field normal to  $B$  can point slightly toward the wall and ions moving normal to  $B$  can strike the wall, causing additional loss of plasma and additional sputtering of walls. This is worth including.

A diverging  $B$  also changes the cross-sectional area of a flux tube from wall to channel center. The wall losses (the  $0.6 n^+ v_s^+$  used above) must be corrected for this area ratio. Because  $B$  is stronger at the wall, the cross sections of flux tubes are smaller there and therefore the loss of ions to the wall is proportionately less.

As shown in the drawing below, one can define an angle  $\psi$  that a normal to  $B$  makes with the wall and calculate the additional wall loss that this causes. (For simplicity, it is assumed that a field line makes the same angle with the inner and outer walls.) One can also allow the channel width to vary — that is,  $W$  becomes  $W(z)$  — and correct the plasma density for the additional expansion. The reduction in the wall losses due to the area being smaller at the wall can be included through an area ratio,  $A(z) \equiv (\text{area at walls})/(\text{area at midplane})$ , which in general will be less than one. Finally, one can recognize that the  $B$ -field strength varies with  $z$ . That is, to solve the

model, first input four functions,  $\psi(z)$ ,  $W(z)$ ,  $A(z)$  and  $B(z)$  that describe the geometry of the channel and the field. The convention is that  $z$  denotes the distance along the midplane of the channel. Distances  $z$  along walls are not physical distances, but mappings of the corresponding midplane distances, with the mapping generated by following  $B$ -field lines.

If the  $B$  field curves as sketched, ion trajectories will not necessarily be exactly normal to  $B$ , even if the  $E$  field is. However, the  $E$  field generally increases with  $z$ , so the ions' direction is primarily affected by the  $E$  field near their location, which is normal to  $B$ . So we assume that the ion "z-velocity" is exactly normal to  $B$ , i.e. directed into the wall at an angle  $\psi$  from tangential.

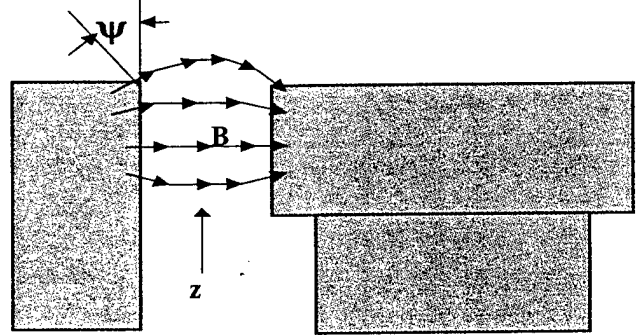
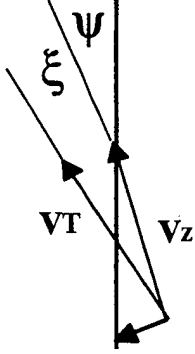


Figure 2 Definition of the angle  $\psi$ .

If this angle were negative, as it is in the lowest field line drawn above, the ion velocity would be angled

away from the wall. This can obviously happen, and would be beneficial, because it would move ions away from the wall, but is also outside the scope of this model, which assumes the plasma has a Gaussian profile (Eqs. [19]–[21]). In this formalism, a negative  $\psi$  would make the wall a source of



If the velocity normal to  $B$  is  $v_z$  and that parallel to  $B$  is  $v_s$ , then the total velocity is  $v_T = \sqrt{v_z^2 + v_s^2}$ . As illustrated to the left, this total velocity makes an angle  $\xi = \tan^{-1}(v_s / v_z)$  with  $v_z$ . The angle between  $v_T$  and the wall is  $(\psi + \xi)$  and the velocity normal to the wall is  $v_\perp = v_T \sin(\psi + \xi)$ . The flux of ions into the wall is  $\Gamma_W = v_\perp n$ . For sputtering, this flux (for each species) strikes the wall at velocity  $v_T$ , at an angle  $(\psi + \xi)$ . But this is not the right wall loss to use in the continuity equations, because  $\Gamma_W$  is the flux per unit area of wall. For continuity, one needs the loss per unit area normal to  $B$ . That flux is  $I = \Gamma_W / \cos(\psi)$ , which replaces  $v_s n$  in the continuity equations.

The other needed modification is the effect on density of a diverging channel, which, to conserve particles, must obey

$$\frac{1}{n} \frac{\partial n}{\partial z} = -\frac{1}{W} \frac{\partial W}{\partial z}.$$

Making these changes in the ion continuity equation [33] gives

$$\frac{\partial n^+}{\partial t} + \frac{1}{W} \frac{\partial}{\partial z} (W n^+ u_z^+) = (\beta n_0 - \gamma n^+) (n^+ + 2n^{++}) - \frac{2v_L^+ n^+ A}{W}$$

where  $v_L^+ \equiv \frac{\sin(\xi^+ + \psi)}{\cos(\psi)} \sqrt{u_z^{+2} + v_s^{+2}}$

and  $\xi^+ \equiv \tan^{-1} \left( \frac{v_s^+}{u_z^+} \right)$

This continuity equation was derived by making the quasi one-dimensional approximation and then setting  $x=0$ . One way in which this is approximate is that it does not exactly conserve particles. To see this, note that the total flux of particles into the two side walls of the channel is  $2(v_L^+)(0.6 n)$ . Integrating across the channel gives the total number of particles,  $0.86(Wn)$ . To conserve particles, one

plasma, which is not physical. Therefore negative values of  $\psi(z)$  will not be input. If  $\psi$  is really negative, as on the lowest field line in the above drawing, it will be set to zero. Note also that  $\psi$  is defined with respect to the wall, not to the vertical.

needs  $(1/n)(dn/dt) = (\text{flux})/(\text{total particles}) = 1.40(v_L^+/W)$ . So the coefficient of the last term in the continuity equation should be 1.4 and not 2. Then the continuity equation becomes,

$$\frac{\partial n^+}{\partial t} + \frac{1}{W} \frac{\partial}{\partial z} (W n^+ u_z^+) = (\beta n_0 - \gamma n^+) (n^+ + 2n^{++}) - \frac{1.4 A v_L^+ n^+}{W} \quad [60]$$

For calculation of sputtering, the flux per unit area of wall is  $= 0.6 n^+ v_L^+ \cos(\psi)$

For the doubly-ionized xenon, [34], the same calculation gives

$$\frac{\partial n^{++}}{\partial t} + \frac{1}{W} \frac{\partial}{\partial z} (W n^{++} u_z^{++}) = \gamma n^+ (n^+ + 2n^{++}) - \frac{1.4 A v_L^{++} n^{++}}{W} \quad [61]$$

where  $v_L^{++} \equiv \frac{\sin(\xi^{++} + \psi)}{\cos(\psi)} \sqrt{(u_z^{++})^2 + (v_s^{++})^2}$  and

$$\xi^{++} \equiv \tan^{-1} \left( \frac{v_s^{++}}{u_z^{++}} \right)$$

and  $A=A(z)$  is the area ratio defined above.



The momentum [35]&[36] and pressure [37]&[38] equations are not changed in form by these effects, although the velocities and pressures predicted by

those equations will change because of the changes in the densities caused by the extra terms in Eqs. [60]&[61].

Making the same additions to the neutral continuity equation [40] gives

$$\frac{\partial n_0}{\partial t} + \frac{1}{W} \frac{\partial}{\partial z} (W n_0 v_{0z}) = -\beta n_0 (n^+ + 2n^{++}) + \frac{1.4 A (v_L^+ n^+ + v_L^{++} n^{++})}{W} \quad [62]$$

Finally, the electron continuity equation, [45] including these effects becomes

$$\frac{\partial n_e}{\partial t} + \frac{1}{W} \frac{\partial}{\partial z} (W n_e v_{ez}) = (\beta n_0 + \gamma n^+) n_e - \frac{1.4 A}{W} (v_L^+ n^+ + 2v_L^{++} n^{++}) \quad [63]$$

### 11.0 Summary of the Model

This completes the formulation. There are twelve variables, namely the four densities and the four  $z$ -velocities for the four species -- the neutral, singly- and doubly charged xenon plus the electrons -- the two ion temperatures, the electron temperature, and the electric field normal to  $B$ . (The neutral temperature is a constant, not a variable.) These twelve variables are defined in the two-dimensional  $(z, t)$  space.

There are also twelve equations, quasineutrality, Eq. [1], the continuity [60]&[61], momentum [35]&[36] and pressure [37]&[38] equations for both ion species, the continuity [62] and diffusion [43] equations for the neutrals, Eq. [44] for the electron drift velocity, Eq. [63] for electron continuity and Eq. [59] that gives the electron temperature implicitly. These equations in turn use the collisional rates, the electron secondary emission coefficient of the wall material, Eq. [50] and the wall sheath voltage drop, Eq. [52].

But it is not necessary to solve this many equations numerically. The quasineutrality condition, Eq. [1] gives the electron density in terms of the ion densities:  $n_e = n^+ + 2n^{++}$ , which can be used to eliminate  $n_e$  from the other equations.

The electron and ion continuity equations, together with quasineutrality, imply

$$\frac{\partial}{\partial z} [W (n^+ u_z^+ + 2n^{++} u_z^{++} - (n^+ + 2n^{++}) v_{ez})] = 0$$

which says that the axial current is conserved. That is,

$$n^+ u_z^+ + 2n^{++} u_z^{++} - (n^+ + 2n^{++}) v_{ez} = \frac{J(t)}{eW}$$

where  $J(t)$  is the total discharge current per unit circumference of the annulus.

This current,  $J(t)$ , is an input to the model, but, as discussed below, one can model an external circuit that is essentially a voltage source by an inversion procedure. Once  $J$  is obtained, this equation, which replaces the electron continuity equation, [63] can be solved for the electron drift velocity:

$$v_{ez} = \frac{n^+ u_z^+ + 2n^{++} u_z^{++} - \frac{J}{eW}}{n^+ + 2n^{++}} \quad [64]$$

and this can be used to eliminate  $v_{ez}$  from all the other equations.

Equation [44] for the electron drift velocity can then be solved for the electric field:

$$E = - B v_{ez} \left[ \left( \frac{v_1 + v_2}{\Omega_e} \right)^2 + \frac{1}{(H_p)^2} \right]^{-1/2} - \frac{1}{en_e} \frac{\partial(n_e k T_e)}{\partial z} \quad [65]$$

Finally, adding the continuity equations [60], [61] and [62], gives

$$\frac{\partial}{\partial t} (n^+ + n^{++} + n_0) + \frac{1}{W} \frac{\partial}{\partial z} [W (n^+ u_z^+ + n^{++} u_z^{++} + n_0 v_{0z})] = 0 \quad [66]$$

which shows that the flux of particles through the thruster is conserved. This can be used instead of Eq. [62], the continuity equation for the neutrals.

With these simplifications, the model consists of eight variables,  $n^+$ ,  $u_z^+$  and  $T^+$ ;  $n^{++}$ ,  $u_z^{++}$  and  $T^{++}$ ;  $n_0$  and  $T_e$ . The electron density and drift velocity, the neutral velocity and the electric field are functions of these primary variables. The eight primary variables obey eight equations, namely [60], [35] & [37] for  $\text{Xe}^+$ ; [61], [36] and [38] for  $\text{Xe}^{++}$ ; [66] for the neutrals and [59] for  $T_e$ . One also needs the functional forms of the collision rates plus  $\delta$  and  $\Phi_W$ , and, finally, a model of the external circuit.

Since the variables are functions of  $z$  and  $t$ , the evident procedure is to store all the needed quantities as functions of  $z$  (e.g. at 1000 points) and advance the system in time. Besides the eight primary variables and four secondary variables ( $n_e$ ,  $v_{ez}$ ,  $v_{0z}$  and  $E$ ), there are also the input functions  $\psi(z)$ ,  $B(z)$ ,  $A(z)$  and  $W(z)$  that describe the channel and  $B$ -field geometry.

While solving these equations, one wants to check that the two conditions mentioned earlier are satisfied, namely (1) that the electric field and electron density are consistent with quasineutrality and (2) that the electron gyroradius is small compared to distances over which the electron density changes. This is conveniently done by defining two ratios,

$$S_1 \equiv \frac{\epsilon_0}{en_e} \frac{\partial E}{\partial z} \quad S_2 \equiv \frac{c_e}{\Omega_e n_e} \frac{\partial n_e}{\partial z} \quad [67]$$

Both of these should be  $< 1$  or the model's assumptions are not satisfied.

## 12.0 Reformulation of the Equations

The next step is to put the equations into a form suitable for numerical solution. To integrate in time, one stores eight variables – the density,  $z$ -velocity and temperature of each ion species, plus the neutral density and the electron temperature – as functions of  $z$ . From these eight, the other four variables –  $v_{0z}$ ,  $E$ ,  $n_e$ , and  $v_{ez}$  – can be calculated, as well as all the  $z$ -derivatives. Then one can calculate the time derivatives of the eight primary variables, and advance the system in time.

Restating the equations for these eight primary variables, one has, from Eq. [60],

$$\frac{\partial n^+}{\partial t} = F_1 \quad [68]$$

where

$$F_1 \equiv -\frac{1}{W} \frac{\partial}{\partial z} \left( W n^+ u_z^+ \right) + (\beta n_0 - \gamma n^+) (n^+ + 2n^{++}) - \frac{1.4 A v_L^+ n^+}{W} \quad [69]$$

And Eq. [35] gives

$$\frac{\partial u_z^+}{\partial t} = -\frac{F_2}{M} \quad [70]$$

where

$$F_2 \equiv \frac{\partial}{\partial z} (E_n^+) + kT^+ \frac{\partial \ln(n^+)}{\partial z} - e E_z + kT_e \frac{\partial \ln(n_e)}{\partial z} - \frac{1}{n_e} \frac{\partial}{\partial z} (kT_e n_e) + \frac{M\beta(n^+ + 2n^{++})n_0(u_z^+ - v_{0z})}{n^+} \quad [71]$$

and

$$E_n^+ \equiv \frac{1}{2} M (u_z^+)^2 + kT^+ + kT_e$$

For  $T^+$ , Eq. [37] gives

$$\frac{1}{T^+} \frac{\partial T^+}{\partial t} - \frac{2}{3n^+} \frac{\partial n^+}{\partial t} = F_3 \quad [72]$$

where

$$F_3 \equiv -u_z^+ \frac{\partial}{\partial z} \ln \left( \frac{kT^+}{(n^+)^{2/3}} \right) + \frac{Mn_0\beta}{3kT^+} \left( 1 + \frac{2n^{++}}{n^+} \right) \left[ (u_z^+ - v_{0z})^2 - \frac{5kT^+}{M} \right] - \gamma(n^+ + 2n^{++}) \quad [73]$$

For  $n^{++}$ , Eq. [61] gives

$$\frac{\partial n^{++}}{\partial t} = F_4 \quad [74]$$

where

$$F_4 \equiv -\frac{1}{W} \frac{\partial}{\partial z} (W n^{++} u_z^{++}) + \gamma n^+ (n^+ + 2n^{++}) - \frac{1.4 A v_L^{++} n^{++}}{W} \quad [75]$$

For the velocity, from Eq. [36],

$$\frac{\partial u_z^{++}}{\partial t} = -\frac{F_5}{M} \quad [76]$$

where

$$F_5 \equiv \frac{\partial}{\partial z} (E_n^{++}) + kT^{++} \frac{\partial \ln(n^{++})}{\partial z} - 2e E_z + 2kT_e \frac{\partial \ln(n_e)}{\partial z} - \frac{2}{n_e} \frac{\partial}{\partial z} (kT_e n_e) + \frac{M\gamma(n^+ + 2n^{++})n^+(u_z^{++} - u_z^+)}{n^{++}} \quad [77]$$

and

$$E_n^{++} \equiv \frac{1}{2} M (u_z^{++})^2 + kT^+ + 2kT_e$$

For  $T^{++}$ , Eq. [38] gives

$$\frac{1}{T^{++}} \frac{\partial T^{++}}{\partial t} - \frac{2}{3n^{++}} \frac{\partial n^{++}}{\partial t} = F_6 \quad [78]$$

where

$$F_6 \equiv -u_z^{++} \frac{\partial}{\partial z} \ln \left( \frac{kT^{++}}{(n^{++})^{2/3}} \right) + \frac{M(n^+ + 2n^{++})n^+\gamma}{3kT^{++}n^{++}} \left[ (u_z^{++} - u_z^+)^2 - \frac{5kT^{++}}{M} + \frac{3kT^+}{M} \right] \quad [79]$$

For the neutral density we have, from Eq. [66]

$$\frac{\partial n^+}{\partial t} + \frac{\partial n^{++}}{\partial t} + \frac{\partial n_0}{\partial t} = -F_7 \quad [80]$$

where

$$F_7 \equiv \frac{1}{W} \frac{\partial}{\partial z} \left[ W (n^+ u_z^+ + n^{++} u_z^{++} + n_0 v_{0z}) \right] \quad [81]$$

Finally, for  $T_e$ , we have, from Eq. [59],

$$\frac{1}{n_e} \frac{\partial}{\partial t} \left( \frac{3}{2} n_e k T_e \right) = -F_8 \quad [82]$$

where

$$\begin{aligned} F_8 &= \frac{v_{ez}}{n_e} \frac{\partial}{\partial z} \left( \frac{3}{2} n_e k T_e \right) + e v_{ez} E + 0.87 v_2 k T_e \\ &\quad + 0.35 \frac{A c_e}{W} e^{\frac{e \Phi_w}{k T_e}} [2k(T_e - \delta T_{\text{sec}}) - (1 - \delta) e \Phi_w] = \\ &= \frac{v_{ez}}{n_e} \frac{\partial}{\partial z} \left( \frac{1}{2} n_e k T_e \right) - e B v_{ez}^2 \left[ \left( \frac{v_1 + v_2}{\Omega_e} \right) + \frac{1}{H_p^2} \right]^{\frac{1}{2}} + 0.87 v_2 k T_e \\ &\quad + \frac{1.4 A}{W} \left[ \frac{n^+ v_s^+ + 2n^{++} v_s^{++}}{(1 - \delta) n_e} \right] [2k(T_e - \delta T_{\text{sec}}) - (1 - \delta) e \Phi_w] \end{aligned} \quad [83]$$

For numerical solution, it is convenient to unscramble the mixed equations in this set, writing

$$\frac{\partial T^+}{\partial t} = T^+ F_3 + \frac{2T^+ F_1}{3n^+} \quad [84]$$

instead of Eq. [72] and

$$\frac{\partial T^{++}}{\partial t} = T^{++} F_6 + \frac{2T^{++} F_4}{3n^{++}} \quad [85]$$

instead of Eq. [78],

$$\frac{\partial n_0}{\partial t} = -F_7 - F_1 - F_4 \quad [86]$$

instead of Eq. [80], and

$$\frac{\partial T_e}{\partial t} = - \frac{T_e}{n^+ + 2n^{++}} (F_1 + 2F_4) - \frac{2F_8}{3k} \quad [87]$$

instead of Eq. [82].

To advance the system in time, starting with the eight primary variables as functions of  $z$ , and therefore their gradients in  $z$ , one must calculate the neutral velocity from Eq. [43] and the collisional rates from the electron temperature. Then one can calculate the eight  $F$ 's and therefore the eight time derivatives needed to advance the system.

In practice, these equations as they stand give difficulties, because they predict sharp gradients that cause numerical problems. This is not physical because particle diffusion smooths the variables. So it makes sense to add diffusion to the model. Taking a mean free path of the order of the channel width, while limiting the diffusion velocities to realistic values gives diffusion coefficients,

$$D^+ = \sqrt{\frac{kT^+}{M}} \left( \frac{1}{n^+} \left| \frac{\partial n^+}{\partial z} \right| + \frac{3}{W} \right)^{-1} \quad D^{++} = \sqrt{\frac{kT^{++}}{M}} \left( \frac{1}{n^{++}} \left| \frac{\partial n^{++}}{\partial z} \right| + \frac{3}{W} \right)^{-1}$$

In the calculation, these were used for the densities, while the coefficients for the velocities and temperatures were taken as one half and one fifth of these rates, respectively.

Mathematically, these additions are an estimate of the higher terms in the velocity-moment expansion that were neglected in the derivation. But to derive them that way, one would have to remember that the system does have walls, ion-ion collisions and fluctuating electric fields in the plasma. Practically, the effect of the diffusion, aside from making the calculation stable, is small. The diffusion terms in one run were increased by 50%. The discharge current did increase, but only by 9%.

### 13.0 External Circuit

The thruster driver was modeled as a voltage source with a series resistance and a parallel capacitance. The discharge current (which the model uses) and the discharge voltage (which the model calculates) imply the current through the capacitor and therefore the derivative of the voltage on the capacitor and discharge. Since the discharge current is input to the model, one needs the change in current that will give the voltage change required by the circuit. In calculating that needed  $dI/dt$ , one must remember that the discharge resistance varies with time. The needed equation is

$$\frac{dV}{dt} = \frac{\partial V}{\partial I} \left| \frac{dI}{dt} + \frac{\partial V}{\partial t} \right|_I \quad \text{or,} \quad \frac{dI}{dt} = \frac{\frac{dV}{dt} - \frac{\partial V}{\partial t} \Big|_I}{\frac{\partial V}{\partial I} \Big|_I} \quad [88]$$

To evaluate this, the program calculates three  $E$  fields and resulting voltages: the  $V$  due to the actual current, the  $V$  due to a slightly different current (for  $\partial V/\partial I|_I$ ) and the  $V$  for the current on the preceding time step (for  $\partial V/\partial t|_I$ ). In practice, the discharge voltage holds constant to within a fraction of a percent, so the power supply is effectively a voltage source.

### 14.0 Boundary Conditions

In practice, one knows the flux,  $n^+ u_z^+ + n^{++} u_z^{++} + n_0 v_{0z}$ . This is not conserved (it can vary if the thruster generates nonsteady flow) but it is constant at the anode, where it equals the gas feed rate. If ions backstream at

the anode (from a downstream ionization zone) their density, velocity and temperature are obtained from extrapolating back to  $z=0$ . Otherwise, we assume that the incoming gas is 1% ionized and 0.1% doubly ionized.

From the total flux and the ion fluxes, one has the anode neutral flux. The neutral density at  $z=0$  is obtained by solving simultaneously for density and velocity to match that flux. Using Eq. [43] for the neutral velocity, taking the gradient at a point  $z_j$  by differencing the density at points  $z_{j+1}$  and  $z_{j-1}$ , and assuming that the gradient at  $z_0=0$  is the same as that at  $z_1$ , one has the flux:

$$Nf(0) \equiv n_0(0)v_{0z}(0) = n_0(0)v_{0s} \frac{\frac{n_0(z_2) - n_0(0)}{2\Delta z}}{\frac{3n_0(0)}{W} + \left| \frac{n_0(z_2) - n_0(0)}{2\Delta z} \right|} \quad [89]$$

giving,

$$n_0(0) = \frac{n_0(z_2) + \frac{Nf(0)}{v_{0s}} \left( \frac{6\Delta z}{W} + 1 \right) + \sqrt{\left[ n_0(z_2) \right]^2 + \frac{2n_0(z_2)Nf(0)}{v_{0s}} \left( \frac{6\Delta z}{W} - 1 \right) + \left[ \frac{Nf(0)}{v_{0s}} \left( \frac{6\Delta z}{W} + 1 \right) \right]^2}}{2}$$

## 15.0 Initial Conditions

The program requires initial profiles for the eight variables. These need not be very accurate, but they must satisfy the boundary conditions. The first runs used simple constant, exponential or Gaussian functions with a few variable parameters. The program is structured so that the results of one run can be used as the starting point for subsequent runs. Although the program evolves the variables in time, there are indications that the initial conditions matter, that the discharge has more than one mode of operation for a given set of operating parameters and that different initial conditions can lead to different steady-state discharge behaviors.

## 16. Solution of the Model

To step in time, the program starts with the eight primary variables and the current, calculates  $E$ ,  $n_e$ ,  $v_{ez}$  and  $v_{0z}$  and then the gradients of these, as well as secondary quantities, such as all the collision and ionization rates. To make the calculation stable, the

program uses either forward or backward differencing, depending on the signs of the velocities.<sup>[22]</sup> Then it calculates the eight  $F$ 's, the diffusion coefficients and finally the time derivatives of the eight primary variables.

The program also integrates  $E$  (for the three different currents) to obtain the discharge voltage and then calculates the current,  $J$ , for the next time step. To model the erosion of the walls by sputtering, it stores, for each ion species, the ion wall flux,  $0.6n^+v_L^+ \cos(\psi)$ , the incident velocity,  $v_L^+$ , and the angle,  $(\psi + \xi)$  that the incident ions make with the tangent to the wall, all as functions of  $z$ . Finally, it also calculates the test quantities  $S_1$  and  $S_2$ .

We have begun exploring the predictions of this model. The following series of current traces show results of runs in which the voltage was varied while the other parameters (magnetic field, channel width, gas feed) were kept constant. As can be seen, at lower voltages, the discharge exhibited oscillatory behavior while higher voltages produced a steadier current.

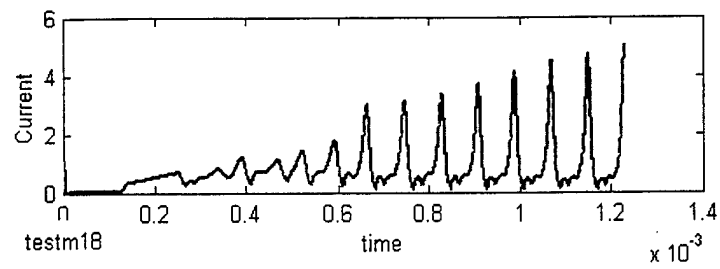


Figure 3 200 V discharge

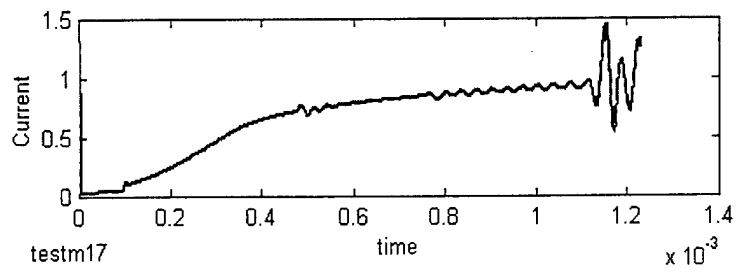


Figure 4 250 V discharge.

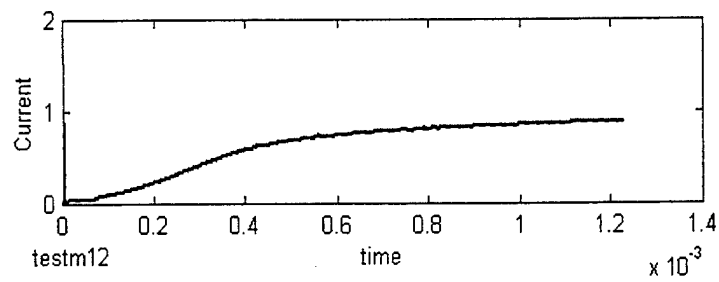


Figure 5 300 V discharge.

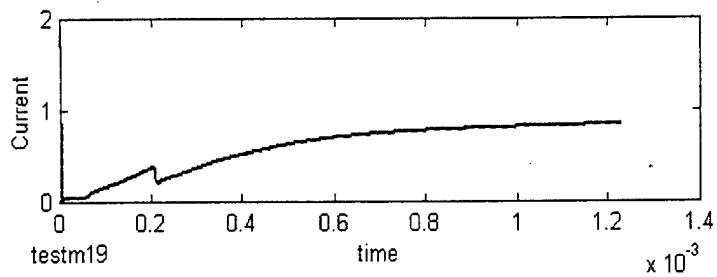


Figure 6 350 V discharge

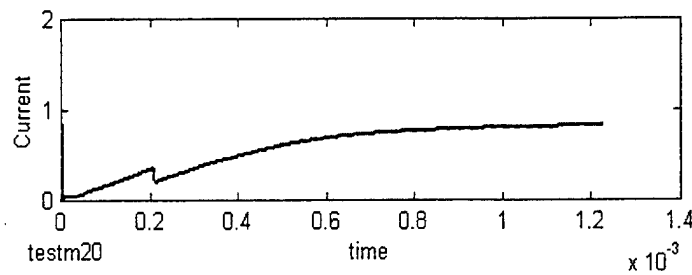


Figure 7 400 V discharge.

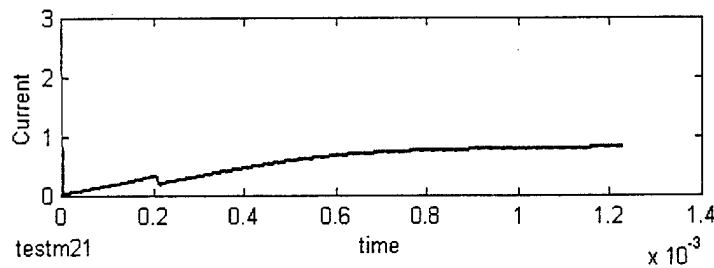


Figure 8 450 V discharge.

In another series of runs, the voltage was kept constant while the width of the discharge channel was varied. The discharges in the narrower channels approached constant current while those in the wider channels exhibited oscillations.

## 17.0 Conclusions

A detailed comparison with experimental data has not yet been made, and we have only begun to explore the parameter space accessible through this model, but the results obtained so far are in general agreement with Hall thruster performance. The success of the derivation described here and the resulting numerical calculations show that a one-dimensional Hall thruster model can include much more of the discharge dynamics than had been done in previous 1-D models. In particular, the ion recombination at the side walls and the effects of a varying channel width and a non-radial magnetic field can all be retained. Although this adds complexity, the resulting simulation is still much simpler and therefore runs much faster than a full two-D code.

This model should be a useful design tool because it predicts both the thruster performance characteristics and the profile of ion bombardment of the side walls

that causes sputtering which limits the operating lifetime. It stores spatial profiles of all the variables at regular times, which should help us understand the nonlinear dynamics of these devices.

## Acknowledgements

The author would like to thank Vlad Hruby for suggesting this analysis, Mary Delichatsios for advice about numerical techniques and David Dvornik for writing the Fortran program. Work was supported by the U.S. Air Force Research Laboratory.

## References

1. C. A. Lentz, "Transient One Dimensional Numerical Simulation of Hall Thrusters," Master's Thesis, MIT, Dept. of Aeronautics and Astronautics, Sept. 1993.
2. A. I. Morozov and V. V. Savelyev, "Numerical Simulation of Plasma Flow Dynamics in SPT," 24<sup>th</sup> Internat. Elec. Propulsion Conf. Moscow, 1995, paper IEPC-95-161 vol. 2, p. 1115-22.



3. V. I. Baranov, et al, "Energy Model and Mechanisms of Acceleration Layer Formation for Hall Thrusters," presented at 33<sup>rd</sup> AIAA/ASME/SAE/ASEE Joint Propulsion and Power Conference, July 6-9, 1997, Seattle WA. Paper AIAA-97-3047.
4. A. Fruchtman, N. J. Fisch, J. Askenazy and Y. Raitses, "Scaling Laws for Hall Thruster Performance," 25<sup>th</sup> International Electric Propulsion Conference, 8/24-8/97, Cleveland, OH, IEPC 97-022.
5. J. P. Boeuf and L. Garrigues, "Low Frequency Oscillations in a Stationary Plasma Thruster," J. Appl. Phys, **84**, Oct. 1, 1998, p. 3541-54.
6. E. Ahedo, P. Martinez and M. Martinez-Sanchez, "Steady and Linearly-Unsteady Analysis of a Hall Thruster with an Internal Sonic Point," 36<sup>th</sup> AIAA/ASME/SAE/ASEE Joint Propulsion Conf. and Exhibit, Huntsville, AL, paper AIAA 2000-3655, July 2000.
7. K. Komurasaki and Y. Arakawa, "Two-Dimensional Numerical Model of Plasma Flow in a Hall Thruster," Journal of Propulsion and Power, **11**, Nov.-Dec., 1995, P.1317-23.
8. J. M. Fife, M. Martinez-Sanchez and J. Szabo, "A Numerical Study of Low-Frequency Discharge Oscillations in Hall Thrusters," presented at 33<sup>rd</sup> AIAA/ASME/SAE/ASEE Joint Propulsion and Power Conf. July 6-9, 1997, Seattle WA. Paper AIAA-97-3052.
9. J. M. Fife, "Two-Dimensional Hybrid Particle-in-Cell Modeling of Hall Thrusters," Master's Thesis, MIT, May 1995.
10. J. M. Fife, "Hybrid-PIC Modeling and Electrostatic Probe Survey of Hall Thrusters," PhD Thesis, MIT, Dept. of Aeronautics and Astronautics, 1998.
11. J. J. Szabo, M. Martinez-Sanchez and J. Monheiser, "Application of 2D Hybrid PIC Code to Alternative Hall Thruster Geometries," AIAA-98-3795, 34<sup>th</sup> AIAA Joint Propulsion Conf. July 1998.
12. J. J. Szabo, M. Martinez-Sanchez and O. Batishchev, "Particle-in-Cell Modeling of Thruster with Anode Layer," IEPC 99-100, 26<sup>th</sup> International Electric Propulsion Conference, October 1999.
13. J. J. Szabo, M. Martinez-Sanchez and O. Batishchev, "Numerical Modeling of the Near Anode Region in a TAL Thruster" 36<sup>th</sup> AIAA/ASME/ASE/ASEE Joint Propulsion Conference. July 2000.
14. J. J. Szabo, "Fully Kinetic Numerical Modeling of a Plasma Thruster," PhD Thesis, MIT, Dept. of Aeronautics and Astronautics, 2001.
15. G. S. Janes and R. S. Lowder, "Anomalous Electron Diffusion and Ion Acceleration in a Low-Density Plasma," Physics of Fluids, **9**, 1966, p. 1115-23.
16. A. I. Morozov et al, "Effect of the Magnetic Field on a Closed-Electron-Drift Accelerator," Sov. Phys. — Technical Physics, **17**, Sept. 1972, p.482-7.
17. E. Y. Choureiri, "Characterization of Oscillations in a Closed-Drift Thruster," 30<sup>th</sup> AIAA/ASME/SAE/ASEE Joint Propulsion Conference, Indianapolis, IN, June, 1994, paper AIAA-94-3013.
18. M. Hirakawa, "Electron Transport Mechanism in a Hall Thruster," 26<sup>th</sup> International Electric Propulsion Conference, Cleveland, Ohio, Aug. 1997, Paper IEPC 97-021.
19. H. Tawara and T. Kato, "Atomic Data and Nuclear Data Tables," **36**, 1987, p. 253-6.
20. F. Reif, "Fundamentals of Statistical and Thermal Physics," McGraw-Hill, 1965, Sect. 7.10, p. 268.
21. L. Spitzer, "Physics of Fully Ionized Gases," Interscience, 1962, Sect. 5.5.
22. D. A. Anderson et al, "Computational Fluid Mechanics and Heat Transfer," McGraw-Hill, 1984, Chapt. 4.